# Three-dimensional morphological characterization of malocclusions with mandibular lateral displacement using cone-beam computed tomography

**Corresponding Author**

a) Roberto L. Velásquez D.M.D., M.S.

Calle 127 No. 19a-28 Cons. 507 Acomedica 1

Bogotá, Colombia 33146

Tel: 571.627.6959, Fax: 571.213.6801

rvtorres8@yahoo.com

Postgraduate research fellow, Department of Oral and Maxillofacial Rehabilitation, Kanagawa Dental University, Yokosuka, Japan.

Associate Professor, Department of Orthodontics, UNICOC, Bogotá, Colombia.

Visiting Professor, Department of Orthodontics, Universidad de Cartagena, Cartagena, Colombia.

**Authors**

b) Jorge C. Coro D.M.D., M.S.

896 South Dixie Highway

Coral Gables, FL 33146

jcc@drcoro.com

Private practice in Orthodontics and Dentofacial Orthopedics, Coral Gables, Fl

Clinical Associate Professor, Department of Orthodontics, University of Florida College of Dentistry, Gainesville, Fl.

Adjunct Faculty, Department of Orthodontics, Nova Southeastern University College of Dental Medicine, Fort Lauderdale, Fl

c) Alejandra Londoño D.M.D.

Carrera 5 # 118 – 10

Bogotá 100121- Colombia

la.londono@unicieo.edu.co

Postgraduate research fellow, Department of Oral and Maxillofacial Rehabilitation, Kanagawa Dental University, Yokosuka, Japan.

Professor, Department of Orthodontics, University CIEO - UNICIEO, Bogotá, Colombia.

d) Susan P. McGorray, PhD

Research Assistant Professor, Department of Biostatistics, University of Florida College of Medicine, College of Public Health and Health Professions.

Gainesville, FL

spmcg@biostat.ufl.edu

e) Timothy T. Wheeler D.M.D., Ph.D.

1395 Center Drive

D1-17

Gainesville, FL 32610

ttgatorwheel@gmail.com

Professor

University of Florida College of Dentistry-Department of Orthodontics

f) Sadao Sato D.M.D., Ph.D.

Kanagawa Dental University

82 Inaoka-Cho, Yokosuka City, Kanagawa 238-8580, Japan.

s.sato@kdu.ac.jp

Institute of Occlusion Medicine, Kanagawa Dental University, Yokosuka, Japan.

# Three-dimensional morphological characterization of malocclusions with mandibular lateral displacement using cone-beam computed tomography


## ABSTRACT

**Objective:** The purpose of this study was to evaluate the morphologic characteristics of MLD malocclusions using 3D imaging.
**Materials and Methods**: MLD characteristics were examined using CBCT data in 40 subjects. A 3D Cephalometric analysis was developed to describe the spatial position of the mandible and temporal bones.
**Results:** Vertical dental heights were shorter and the posterior occlusal plane (POP) presented a steeper sagittal inclination on the shifted side than on the contralateral side. ($p<0.01$). The MLD was related to a superiorly inclined POP Cant in the same direction ($r=0.82$; $p<0.01$). The shifted side condyle was dislocated medially and was smaller. Temporal bone sagittal inclination showed a more forward and medial inclination on the contralateral side ($p<0.01$).
**Conclusions:** A unilateral decrease in the vertical height of the dentition and the subsequent steeper occlusal plane inclinations correlated with 1) mandibular rotational displacement and condylar lateral displacement, 2) mandibular and condylar morphologic changes 3) changes in temporal bone position


Key Words Facial Asymmetry; Malocclusion; Mandible; Vertical Dimension; Occlusal Plane

# Three-dimensional morphological characterization of malocclusions with mandibular lateral displacement using cone-beam computed tomography


## ABSTRACT

**Objective:** The purpose of this study was to evaluate the morphologic characteristics of MLD malocclusions using 3D imaging.
**Materials and Methods**: MLD characteristics were examined using CBCT data in 40 subjects. A 3D Cephalometric analysis was developed to describe the spatial position of the mandible and temporal bones.
**Results:** Vertical dental heights were shorter and the posterior occlusal plane (POP) presented a steeper sagittal inclination on the shifted side than on the contralateral side. ($p<0.01$). The MLD was related to a superiorly inclined POP Cant in the same direction ($r=0.82$; $p<0.01$). The shifted side condyle was dislocated medially and was smaller. Temporal bone sagittal inclination showed a more forward and medial inclination on the contralateral side ($p<0.01$).
**Conclusions:** A unilateral decrease in the vertical height of the dentition and the subsequent steeper occlusal plane inclinations correlated with 1) mandibular rotational displacement and condylar lateral displacement, 2) mandibular and condylar morphologic changes 3) changes in temporal bone position


Key Words Facial Asymmetry; Malocclusion; Mandible; Vertical Dimension; Occlusal Plane


## INTRODUCTION

Many types of malocclusions are associated with some degree of facial asymmetry, which makes detection of mandibular lateral displacements (MLD) important. Malocclusions associated with MLD are commonly characterized as having a deviation of the chin from the facial midline because of a mandibular shift to one side. In addition, other morphologic features of MLD may include a dental midline discrepancy, the presence of a crossbite in the posterior region and frequent association with articular dysfunction. [1-6] A malocclusion accompanied by MLD is a difficult orthodontic challenge even if treated by surgical means, not only because of the skeletal asymmetry present in such cases but also due to the lack of understanding of the morphological characteristics involved in these types of malocclusions.

A number of studies have revealed a relationship between occlusion and growth, [7-9] and some have reported adaptive growth of the mandible or the condyles when undergoing changes in occlusal conditions. [8] Other studies established an association between mandibular deviations caused by occlusal changes and jaw growth,

demonstrating the functional capacity of the condyles to adapt to changes in mandibular position. [8, 9] Therefore, the dentofacial complex demonstrates the ability to respond to functional demands in occlusal arrangements. [9, 10] The functional displacement that results from the adjustment of the dento-alveolar and skeletal components of the face maintains the orofacial region's structural and functional homeostasis. [11, 12]

Different studies have proposed an association between occlusal deviations and facial growth, mainly in patients with mandibular asymmetry, transverse inclination of the occlusal plane and differing muscle activity of both sides caused by occlusal vertical dimension discrepancies. [13-16] The vertical occlusal height has shown a particular influence on the cant of the posterior occlusal plane, thus affecting mandibular position and function in several skeletal malocclusions. [15, 17] These bi-dimensional studies suggest that it is important to consider the association between the vertical and transverse positions of the mandible with the vertical height of the posterior teeth (posterior vertical dimension) playing a major role in understanding MLD malocclusions.

The recent development of cone-beam computed tomography (CBCT) has improved craniofacial skeletal evaluation. The high accuracy of 3D CBCT imaging provides an accurate representation of the craniofacial structures necessary for the study of MLD malocclusions. [18, 19]

The purpose of this retrospective 3D-CBCT study is to determine the morphologic characteristics of MLD malocclusions. The null hypothesis is that bilateral vertical differences in the posterior occlusal plane are not correlated with MLD.

## MATERIAL AND METHODS

### *MLD Cases Used in This Study*

This study was approved by the University of Florida Institutional Review Board for the Protection of Human Subjects (IRB-01). 3D data was obtained from CBCT scans of patients at a private orthodontic practice as part of their pre-treatment diagnostic records.

The retrospective convenience sample consisted of 40 patients (26 males, 14 females) with an average age of 23.4 years (SD, 6.6 years) with minimum age of 14.9 years and maximum age of 44.6 years. The sample was selected from a database of pretreatment clinical examination records using study models, photographs, and CBCT scans. Subjects were of diverse ethnic backgrounds and were selected based on the following inclusion criteria: (1) MLD observed by chin deviation of 2.4 degrees or more as assessed by the angle made by the line ANS-Men and the midsagittal reference plane (MSRP) (N-ANS-Ba), (2) non-coincident right and left molar relationships as well as non-coinciding dental midlines; (2) all permanent teeth erupted, including second molars; (3) absence of pathologic conditions that affect the TMJ. Pathologic conditions that excluded a patient from participating included congenital disorders such as hemifacial microsomia, condylar hyperplasia, rheumatoid arthritis, and osteoarthritis.

### *3D-CBCT*

The CBCT scans were performed with a Kodak 9500 Cone Beam (90 kW, full field of view: 200 × 184mm, 0.3mm voxel resolution and 2-15 mA) and were imported into Anatomage Dental's InVivo software, version 5.2.4 (San Jose, CA, USA) for rendering. This program was used to visualize the slices and the 3D images obtained from the CBCT scans. The cases were anonymized by removing all patient identifiers. All patients included in the sample signed the consent to use records section in the Informed Consent Form provided by the American Association of Orthodontists.

### *Reference Plane, Landmarks, and Measurements*

A 3D cephalometric analysis was developed with 40 different landmarks that were accurately selected in the 3D volume and then refined in the axial, coronal, and sagittal slices using the slice locator feature in the software (Table 1). Each landmark was selected using an Apple optical mouse on a 21-inch iMac (Apple). Ten angular and 15 linear 3D cephalometric measurements (Table 3) were obtained by InVivo software. A single calibrated operator (RV) selected the anatomical landmarks and performed the cephalometric analysis for the 40 subjects. The angular and linear 3D cephalometric measurement data was exported from the InVivo software to Microsoft Excel files with the corresponding identification number. The measurements were then exported from the Excel files to R software (http://www.r-project.org) for statistical analysis.

Six 3D reference planes were defined and established (Fig 1), (Table 2). To define the 3D curved surface of the maxillary occlusal plane, it was divided into anterior and posterior planes as described by Okuhashi et al. [20] The anterior occlusal plane (AOP) is defined by the most mesial incisal point of the maxillary left central incisor (U1) and the right and left second premolar buccal cusp tips (U5R, U5L). In order to measure its effect on the right and left sagittal views, two lines were created from the point U1 to the U5R and U5L. These were defined as AOP-R and AOP-L. A third line constructed from UR5 to UL5 was named AOP-cant and was used to measure its effect on the coronal plane. The posterior occlusal plane (POP) was also defined by three points, the first being a computer generated medial (mean) point between the right and left second premolar buccal cusp tips (Premed U5). The right and left second molar disto-buccal cusp tips (U7R, U7L) complete the definition. In order to measure its effect on the right and left sagittal views, two lines were created from the point Premed U5 to the U7R and U7L. These horizontal planes were projected to the MSRP, measured in 2D. (Fig 5) To measure this plane's effect in the coronal views, a third line was constructed from U7R to U7L and was named the POP-cant. Positive values of AOP-cant and POP-cant indicated superior inclination toward the left side (Fig 2).

Using the same projection technique, the vertical dental height was measured from the right and left second molar disto-buccal cusp tips and the palatal plane (U7-PP), the right and left second premolar buccal cusp tips and the palatal plane (U5-PP), and the

most mesial and incisal point of the maxillary left central incisor and palatal plane (Fig 5).

To determine the spatial position of the mandible and temporal bone in the coordinate system, several landmarks similar to those from conventional 2D analyses were used and several new ones were created. The landmarks that describe their anteroposterior, vertical and transverse spatial position are listed in (Table 1).

The MLD was defined as the angle made by the line ANS-Me with the MSRP. This measurement was projected onto the vertical reference plane (VRP). A positive value indicated the MLD was to the left side and a negative value to the right side. The absolute value of the MLD ranged from 2.4 to 12.7 degrees (Fig 2).

The MSRP was used as the main reference plane since the craniofacial complex is a three-dimensional object that is by no means perfectly symmetrical. Finding the geometric midline in such a non-perfect structure can be arbitrary at best and thus not feasible. The anatomical landmarks (Ba, S and ANS) can be accurately selected and reproduced in the rendered 3D volumes and thus it was considered a valid representation of the skeletal midline. Another factor that was taken into account is that ANS denotes the position of the maxilla in space, which is indicative of the relative position of the midface. The position of the midface appears to play a significant role in MLD malocclusions. It has been observed that 36% of facial asymmetries have midface asymmetries and 75% have lower face asymmetries. [21] When analyzing and quantifying the degree of MLD, the main interest in this study was the maxillo-mandibular relationship and thus the angle made by the line ANS-Me and the MSRP is a reasonable method of assessing the transverse discrepancy between the maxilla and the mandible.

As previously noted the term cant is used to describe the lines or planes that are measured on the coronal view. To describe the angular position of the mandible from this perspective, the gonial cant (Go-cant) was defined as the line GoR and GoL in reference to FH. Positive values of Go-cant indicated superior inclination toward the left side (Fig 2).

Three different landmarks were identified on both the left and right temporal bones: porion (Po), temporoparietal point (TP), and sphenotemporal point (ST). The Po, TP and ST landmarks were used to measure the temporal bone inclinations in the sagittal and coronal planes. The distance from landmarks, TP and ST were measured perpendicular to the MSRP (Fig 3 and 4). To describe the angular position of the temporal bone on the coronal view, mastoid cants (Ma-cant) was defined as the line MaR and MaL in reference to FH. A positive Ma-cant value indicated superior inclination toward the left side (Fig 2).

Three condylar landmarks were also selected in the reconstructed 3D volume and refined in the axial, coronal and sagittal slices. The center of the condyles (CCo) were selected on the sagittal view. The most convex point of the lateral pole (lateral pole) and the most convex point of the medial pole (medial pole) were selected on the coronal view. The most convex point of the anterior pole (anterior pole) and the most convex point of the posterior pole (posterior pole) were selected in the axial view. The size of the condyle

(length and width) was measured from lateral pole to medial pole and from anterior pole to posterior pole respectively (Fig 6). The Bonwill triangle, which consists of the intercondylar (CCoR-CCoL) distance and of both right and left CCo points and the lower incisal (L1) point, was calculated (Fig 7). The 3D mandibular position was established as the distance from condylion (Cd) to MSRP, VRP and horizontal reference plane (HRP) (Fig 8). Mandibular body length (MdL) was measured from the right and left gonion (Go) to the pogonion (Po). Ramus height (RamHt) was measured from the condylion (Cd) to the right and left gonion (Go) and mandibular length was measured from the condylion (Cd) to the pogonion (Po) (Fig 9).

***Statistical analysis***

The same investigator located the same landmarks and measured the same items on ten randomly selected CBCT images as described above at a 4-week interval to assess the intra-observer reproducibility, where the measurement error both for angular as for linear measures were lower than 0.99mm and/or 0.99 degrees. This was estimated using the Dahlberg test and the measurement repeatability was estimated by the Houston test (greater or equal to 83%) and P> 0.1, which indicates that there was no significant difference between the initial and final measurements and that the errors were less than the measurement unit (Table 4).

Sample size considerations were based on the ability to detect correlation between measurements and testing whether paired differences were significantly different from zero. For correlation, using a two-sided test with level of significance set at 0.05 and a sample size of 40 provide~~s~~ adequate (0.80) power to detect correlations of 0.43 or greater, and excellent power (0.90) to detect correlations of 0.49 or greater. Correlations of this magnitude would be of clinical interest. Paired t-tests would be used to compare differences between the shifted and contralateral sides. With a sample size of 40, using a two-sided test, with level of significance 0.05~~,~~ we have adequate power (0.80) to detect a difference between sides of 0.45 standard deviation units and excellent power (0.90) to detect a difference of 0.51 standard deviation units. Differences of this magnitude would be of clinical interest.

Statistical analyses were performed with Microsoft Excel 2013 and the R V3.02 2013 program for Windows (Bell Laboratories (formerly AT&T, now Lucent Technologies). Descriptive statistics including the means, standard deviations, minimums and maximums for all variables were calculated. The Shapiro Wilk test was used to verify that all measurements exhibited a normal distribution (P >0.05) in addition to standard descriptive statistical calculations. The Student's t-test was used to detect significant differences in outcome measures between the two groups, shifted and contralateral side in MLD (Tables 5), and the statistical significance levels were established at P <0.05. The Spearman's coefficient (test) and Pearson product-moment correlation coefficients were used to establish the different associations that could be present between variables linked

to MLD malocclusion (AOP-cant, POP-cant, Go-cant and Ma-cant). The statistical significance of correlation was set at $P < 0.05$ (Table 6).
The data was analyzed in the total sample and no significant differences were found in the variables between the sexes.

## RESULTS

In every subject, a greater distal occlusion was found on the shifted side than on the contralateral side. (Table 7) A unilateral Class III relationship was found on the opposite side of the mandibular displacement in seven subjects with right displacement and nine subjects with left displacement, all with posterior crossbites. Twelve subjects had a bilateral Class III relationship and severe mandibular prognathism with posterior crossbite. A unilateral Class II relationship was found on the shifted side in five subjects with left displacement and two of them with posterior crossbite and seven subjects with right displacement and three of them with posterior crossbite.

### *MLD and Occlusal Planes*

On the frontal view, the results demonstrated a low and high correlation of 0.514 and 0.822, respectively, between the AOP-cant and POP-cant inclination and the MLD. The superiorly inclined POP-cant was associated with the MLD in the same direction. There was a high correlation of 0.833 between the MLD and the Go-cant inclination. The POP-cant and Ma-cant showed negative correlation coefficient of -0.613. The MLD and Ma-cant showed negative correlation coefficient of -0.787 (Table 6).

The shifted and contralateral side presented a significant difference in the AOP and POP inclination. There was a significantly steeper POP on the shifted side compared to that on the contralateral side (Table 5).

### *Mandibular Morphology*

As seen in Table 5, mandibular body length (MdL) is larger on the shifted side than on the contralateral side, although condylion-pogonion (Cd-Pg) length is larger on the contralateral side than on the shifted side. The ramus height (RamHt) is also larger on the contralateral side than on the shifted side. The distances between the lower incisal point (L1) to both shifted side and contralateral side center of the condyle (CCo) were the same as the CCoR-CCoL distance.

### *Condylar Posture and Morphology*

Comparison of the condylar size in the shifted and contralateral sides showed that length and width of the shifted side of the condyle was significantly smaller than that of the contralateral side (Table 5). Condylar position is more medial on the shifted side than on the contralateral side.

***Temporal Bone Posture***

Temporal bone sagittal inclination (Po-TP-VRP) showed a more forward inclination on the contralateral side than on the shifted side. Transversal temporal bone posture (ST-MSRP and TP-MSRP) showed a more lateral inclination on the shifted side than on the contralateral side (Table 5). Vertical temporal bone position was higher on the contralateral side as determined by the Ma-cant.

**DISCUSSION**

Forty patients were examined using 3D-CBCT scans to obtain a better understanding of the morphological features of malocclusions with MLD. The 3D cephalometric analysis developed for this investigation provided the ability to select the anatomical landmarks on the reconstructed three-dimensional models of the patients within the sample without the distortions and superimposition of other structures observed in 2D radiographs. [17, 18] Although many of the measurements used were borrowed from conventional 2D analyses and were projected on to their respective reference planes, this method afforded the ability to better describe the bilateral aspects of craniofacial morphology.

In this study, MLD patients showed a correlation between the POP-cant and AOP-Cant inclination with the MLD. The results suggest that in MLD malocclusions the AOP-cant and POP-cant were more superiorly inclined on the shifted side than on the contralateral side. Decreased dentoalveolar vertical heights, were also observed on the shifted side compared with the contralateral side (Table 5). This indicated less maxillary eruption on the shifted side than on the contralateral side. These findings suggest that the inclination of the OP is associated with a decrease or increase in the dental vertical height on one side and represents a potential risk factor for lateral mandibular shift to the side that presents with less vertical dimension. This coincides with Schudy's [22] assertion that the occlusal planes are dependent on the differential vertical development of the dentoalveolar processes. The inclination of the Go-cant also indicated significant correlation with MLD with a correlation coefficient of 0.833. In addition to these, analysis of the relationship of the POP-cant and Go-cant showed a high correlation with a correlation coefficient of 0.835, indicating that the occlusal plane inclination was strongly related to a 3D shift of the mandible toward the side with less vertical dimension (Table 6). Ishizaki et al [23] and Coro et al [15} showed similar results in a previous bi-dimensional study and 3-dimensional study respectively.

On the sagittal view the results were in agreement with previous 2D findings, the AOP and POP inclination presented a significant difference between the shifted and the contralateral side (Table 5). A shift of the condyles to the contralateral side was also observed. A negative correlation coefficient of -0.787 and -0.613, respectively (Table 6) between Ma-cant and MLD and POP-cant was observed. This finding suggests that the temporal bone position appears to play a role in these complex malocclusions; there was

a greater lateral inclination on the shifted side than on the contralateral side and different sagittal inclinations were observed. This relationship of the POP-cant and MLD to the temporal bone is a significant finding that can help to explain the altered cervical curvature and head posture observed in many MLD patients [24-25]. Brodal found that there tends to be less variation in natural head posture in the coronal axis. [26] It is possible that since the temporal bones house the organs of equilibrium, they provide the sensory input for the spatial orientation of the head. [27] The relationship of head posture to the Ma-cant is an interesting topic that needs further investigation.

Sanders et al [28] showed mandibular asymmetry among Class II subdivision patients with the mandible posteriorly positioned in the Class II side. Williamson and Simmons, [29] showed that 70% of patients with a unilaterally short mandible also had a greater distal occlusion on the shifted side. The results of this study are in agreement with their findings. Although the MdL was larger on the shifted side, the Cd-Pg length and RamHt were shorter on the same side. As in previous studies, [30] the Bonwill triangle proved to be equilateral. The distances between the L1 to both shifted side and contralateral side CCo were the same as the CCoR-CCoL distance. This demonstrates that the dentition maintains symmetry, even when the mandible is asymmetric and shifted laterally.

The results presented here indicate that MLD is not just a consequence of a simple mandibular lateral shift; on the contrary, it encompasses several additional complex components. It was observed that the mandible was three-dimensionally rotated with a tilt of the Go-cant along with condylar displacement to the opposite side. The condyles showed significant differences in size between the two sides and more importantly the two temporal bones also showed significant differences in their sagittal angulation, their transverse and vertical position.

***Clinical implications***

In a previous study, Ishizaki [23] proposed two different possible mechanisms that explained the development of MLD. First, an occlusal fulcrum on the posterior molar of the higher side could develop because of the vertical height discrepancy of the dentition between both sides. Second, a mandibular shift due to the lack of symmetrical occlusal guidance could create a unilateral chewing habit. As a reaction, the chewing side would receive a higher occlusal load that prevents the eruption of teeth on that side. The results of this study are in agreement with the first proposed mechanism for the development of MLD. The internal derangement of the TMJ or differential condylar growth could be an outcome of the mandibular displacement with the tilting OP and the consequent condylar displacement. Future studies are needed to investigate the second possible mechanism, which this study did not address.

Orthodontic occlusal reconstruction aims to correct mandibular position by increasing the vertical dimension on the shifted side so that the mandible adapts anteriorly on this

side and by decreasing the vertical dimension on the contralateral side so that it adapts posteriorly. The occlusal plane cant is therefore reconstructed resulting in the correction of the chin position. [14] Previous studies [14, 31] indicate that controlling the OP and the change in dento-alveolar vertical dimension during orthodontic treatment show concomitant improvement in mandibular position. This allows for proper function of the stomatognathic system and in most patients, correction of the abnormal growing process. Future research should aim at comparing a sample of MLD patients to a sample of non-MLD subjects.

## CONCLUSIONS

The results of this study help to explain the many elements involved in MLD malocclusions; from discrepancies in occlusal vertical dimension and occlusal plane inclination to facial asymmetry, changes in condylar morphology and temporal bone posture. Decreased vertical height of the dentition on one side and the subsequent different occlusal plane inclinations are correlated with 1) mandibular rotational displacement and condylar lateral displacement, 2) changes in condylar and mandibular morphology and 3) changes in temporal bone position.

It is essential to consider these aspects of MLD malocclusion in the treatment protocol and to approach these cases through the differential control of the occlusal vertical dimension and the occlusal plane on both sides.

### Disclaimer Statements

**Contributors** RV- carried out the study, collected the CBCT images drafted the manuscript and made the measurements. JC - provided the CBCT records and was instrumental in data collection and development of the 3-D analysis. He collaborated on the design, and editing of the manuscript. AL - was involved in data analysis, reviewing the manuscript. SM - provided the statistical analysis and assisted with interpretation of the data. TW - was an advisor on the study and involved in the manuscript preparation as well as guidance throughout the study on design and implementation. SS - was a primary advisor on the study and was involved in the design of the study and data analysis, as well as manuscript preparation.

**Funding** No funding was obtained for this study.

**Conflicts of interest** The authors declare no potential conflicts of interest to report

## ACKNOWLEDGMENTS

The authors thank Dr. Michael Spoon and Dr. Andrea Velandia for their assistance in the preparation of this manuscript and Dr. Gerardo Ardila for his assistance with statistics.

## REFERENCES

[1] Lundstrom A. Some asymmetries of the dental arches, jaws, and skull, and their etiologic significance. *Am J Orthod* 1961;47:81–106.

[2] Fisher B. Asymmetries of the dentofacial complex. *Angle Orthod* 1954;24:179–92.

[3] Inui M, Fushima K, Sato S. Facial asymmetry in temporomandibular joint disorders. *J Oral Rehabil* 1999;26:402–6.

[4] Fushima K, Odaira Y, Saito N, et al. Dental asymmetry in facial asymmetry. *Bull Kanagawa Dent Coll* 1998;26:15–21.

[5] Fushima K, Akimoto S, Takamoto K, et al. Incidence of temporomandibular disorders in patient with malocclusion. *J Jpn Soc TMJ* 1989;1:40–50.

[6] Fushima K, Sato S, Suzuki Y, et al. Horizontal condylar path in patients with disk displacement with reduction. *J Craniomand Pr*act 1994;12:78–86.

[7] Isaacson RJ, Zapfel RJ, Worms FW, et al. Some effects of mandibular growth on the dental occlusion and profile. *Angle Orthod* 1977;47:97–106.

[8] McNamara JA Jr. Neuromuscular and skeletal adaptations to altered function in the orofacial region. *Am J Orthod* 1973;64:578–606.

[9] Harvold EP. The role of function in the etiology and treatment of malocclusion. *Am J Orthod* 1968;54:883–98.

[10] McNamara JA Jr, Bryan FA. Long-term mandibular adaptations to protrusive function: an experimental study in Macaca mulatta. *Am J Orthod Dentofacial Orthop* 1987;92:98–108.

[11] Petrovic, A., Stutzman J. *The biology of occlusal development. Monograph 6. Craniofacial Growth Series*. Ann Arbor: Center for Human Growth and Development, University of Michigan; 1977.

[12] Elgoyhen JC, Moyers RE, McNamara JA, et al. Craniofacial adaptation of protrusive function in young rhesus monkeys. *Am J Orthod* 1972;62:469–80.

[13] Fushima K, Akimoto S, Takamoto K, et al. Morphological feature and incidence of TMJ disorders in mandibular lateral displacement cases. *J Jpn Orthod Soc* 1989;48:322–8.

[14] Sato S, Takamoto K, Fushima K, et al. A new orthodontic approach to mandibular lateral displacement malocclusion. Importance of occlusal plane reconstruction. *Dent Jpn* 1989;26:81–5.

[15] Coro J, Velasquez R, Coro I, Weeler T, et al. Relationship of maxillary 3-dimensional posterior occlusal plane to mandibular spatial position and morphology. *Am J Orthod Dentofacial Orthop* 2016;150:140-52

[16] Akimoto S, Fushima K, Sato S, et al. Masticatory muscle activity of the facial asymmetry cases. Effects of the different combination of bite blocks. J Jpn Orthod Soc 1994;53:632–640.

[17] Fushima K, Kitamura Y, Mita H, et al. Significance of the cant of the posterior occlusal plane in Class II division 1 malocclusions. *Eur J Orthod* 1996;18:27–40.

[18] Baumgaertel S, Palomo J, Hans M. Reliability and accuracy of cone-beam computed tomography dental measurements. Am JOrthod Dentofacial Orthop 2009;136:19-2518

[19] Damstra J, Fourie Z, Ren Y. Evaluation and comparison of posteroanterior cephalograms and cone beam computed tomography imagesfor detection of mandibular asymmetry. Eur J Orthod 2013;35:45-50.

[20] Okuhashi S, Basili C, Sasaguri K, et al. Three-Dimensional Computer Tomographic Analysis of the Influence of the Cant of the Occlusal Plane in Different Craniofacial Morphology. Bull Kanagawa Dent Coll 2011;39:89–99.

[21] Severt T, Proffit W. The prelevanc of facial asymmetries in the dentofacial deformities population at the University of North Carolina. Int J Adult Orthodon Orthognath Surgery 1997;12:171-176.

[22] Schudy F. Cant of the occlusal plane and axial inclination of teeth. Angle Orthod 1963;33:69-82.

[23] Ishizaki K, Suzuki K, Mito T, et al. Morphologic, functional, and occlusal characterization of mandibular lateral displacement malocclusion. *Am J Orthod Dentofacial Orthop* 2010;137:454.e1–9; discussion 454.e1-454.e9.

[24] Huggere J, Pirttiniemi P, Serlo W. Head posture and dentofacial morphology in subjects treated for scoliosis. Proc Finn Dent Soc 87:151–158

[25] Nakashima, A., Nakano, H., Yamada, T. et al. The relationship between lateral displacement of the mandible and scoliosis. *Oral Maxillofac Surg. 2017 Mar;21(1):59-63. doi: 10.1007/s10006-016-0607-9.*

[26] Brodal A, Pomperiano O. Basic aspects of central vestibuar mechanisms.Amsterdam, The Netherlands: Elsevier Science; 1972.

[27] Fleiss J. The design and analysis of clinical experiments. Hoboken,NJ: Wiley-Interscience; 1986.

[28] Sanders DA, Rigali PH, Neace WP, et al. Skeletal and dental asymmetries in Class II subdivision malocclusions using cone-beam computed tomography. *Am J Orthod Dentofacial Orthop* 2010;138:542.e1–.

[29] Williamson EH, Simmons MD. Mandibular asymmetry and its relation to pain dysfunction. *Am J Orthod* 1979;76:612–7.

[30] Fukoe H, Basili C, Slavicek R, et al. Three-dimensional analyses of the mandible and the occlusal architecture of mandibular dentition. Int J Stomatol Occl Med. 2012;5:119–125.

[31] Sato S, Kim JI, Kim KM, et al. Significance of early orthodontic treatment of malocclusion with dysfunction in the craniomandibular system. *Bull Kanagawa Dent Coll* 2004;32:37–48.

**Table 1.** Description of the 3D cephalometric landmarks used in this study.

| *Landmark* | *Definition* |
|---|---|
| S (Sella) | The midpoint of the pituitary fossa in the midsagittal plane. |
| N (Nasion) | The middle point of the frontonasal suture in the frontal plane. |
| Ba (Basion) | Anterior-inferior margin of the foramen magnum. |
| PoR-PoL (Porion) | Most superior point of the right (PoR) and left (PoL) outer acoustic meatus. |
| OrR-OrL (Orbital) | The most inferior point on the infraorbital rim of the maxilla. |
| STR, STL (Sphenotemporal point) | The most anterior point on the external surface of the right (STR) and left (STL) sphenotemporal suture. |
| TPR, TPL (Temporoparietal point) | The most superior point on the external surface of the right (TPR) and left (TPL) temporoparietal suture. |
| MaR-MaL (Mastoid) | The lowest point of the mastoid process of the temporal bone. |
| ANS (Anterior nasal spine) | The most anterior point of the premaxillary bone in the sagittal plane. |
| PNS (Posterior nasal spine) | The most posterior point of the palatine bone in the midsagittal plane. |
| A (A point) | The deepest point in the anterior outline of the maxilla between supradentale and ANS in the midsagittal plane. |
| U1 (Upper interincisor point) | The most incisal point between the two upper central incisors. |
| U5R, U5L (2nd premolar) | Tip of the buccal cusp of the second upper right (U5R) and left (U5L) premolar. |
| Premed (Mean 2nd premolar) | Calculated 3D medial (mean) point between U5R and U5L. |
| U7R, U7L (2nd molar) | Tip of the distobuccal cusp of the upper right (U7R) and left (U7L) second molar. |
| B (B point) | The deepest point in the anterior outline of the mandible between infradentale and pogonion in the sagittal plane. |
| Pg (Pogonion) | The most anterior point in the mandibular chin area in the sagittal plane. |
| Me (Menton) | The most inferior point in the mandibular chin area in the sagittal plan. |
| GoR and GoL (Gonion) | The midpoint of the right (GoR) and left (GoL) angles of the mandible, formed by the inferior border of the corpus and posterior ramus border. |
| CdR-CdL (Condylion) | Most posterosuperior point of the right (CdR) and left (CdL) mandibular condyle. |
| CdLR-CdLL (Condylion lateral pole) | The most lateral point of the right (CdLR) and left (CdLL) condylar head. |
| CdMR-CdML (Condylion medial pole) | The most medial point of the right (CdLR) and left (CdLL) condylar head. |
| CdAR-CdAL (Condylion anterior pole) | The most anterior point of the right (CdLR) and left (CdLL) condylar head. |
| CdPR-CdPL (Condylion posterior pole) | The most posterior point of the right (CdLR) and left (CdLL) condylar head. |
| CCoR-CCoL (Center of condyle) | The 3D central point of the right (CCoR) and left (CCoL) mandibular condyle. |
| L1 (lower interincisor point) | The most incisal point between the two lower central incisors. |

**Table 2.** Definition of 3D planes used in the analysis

| *Plane* | *Definition* |
|---|---|
| MSRP (Midsagittal reference plane) | Plane through Basion, Nasion, and ANS. |
| AH (Anatomical Horizontal) | Plane that contains posterior – anterior vector (PoR to OrR) that is perpendicular to the midsagittal reference plane (MSRP) |
| FRP (Frontal reference plane) | Plane through Nasion and perpendicular to the midsagittal reference plane (MSRP) and anatomical horizontal (AH). |
| HRP (Horizontal reference plane) | Plane through Sella and perpendicular to the midsagittal reference plane (MSRP) and frontal reference plane (FRP). |
| VRP (Vertical reference plane) | Plane through Sella and perpendicular to the midsagittal reference plane (MSRP) and anatomical horizontal (AH). |
| AOP (Anterior occlusal plane) | Plane defined by 3 landmarks: upper Interincisor point (U1), right (U5R) and left (U5L) second premolar. |
| POP (Posterior occlusal plane) | Plane defined by 3 landmarks: medial second premolar (Premed), right (U7R) and left (U7L) second molar. |

**Table 3.** Definition of the Cephalometric angular and linear measurements used in this study.

| *Measurement* | *Definition* |
|---|---|
| Angular measurements: | |
| STTP-MSRP (temporal frontal inclination) | Mean angle between left and right ST-TP lines and the midsagittal reference plane (MSRP). |
| PoTP-VRP (temporal sagittal inclination) | Mean angle between left and right Po-TP lines and the vertical reference plane (VRP). |
| AOPL-FH | 3D angle between AOPL and FH reference plane. |
| AOPR-FH | 3D angle between AOPR and FH reference plane. |
| POPL-FH | 3D angle between POPL and FH reference plane. |
| POPR-FH | 3D angle between POPR and FH reference plane. |
| CdAxis-VRP | Mean angle between left (CdLL-CdML) and right (CdLR-CdMR) |
| MLD (mandibular lateral displacement) | ANS-Men line and MSRP (Ba-Na-ANS) |
| Go-cant (gonial cant) | 3D angle between GoR-GoL line and FH reference plane |
| Ma-cant (mastoid cant) | 3D angle between MaR-MaL line and FH reference plane |
| Linear measurements: | |
| ST-MSRP | The perpendicular distance between left and right ST and the MSRP. |
| TP-MSRP | The perpendicular distance between left and right TP and the MSRP. |
| U1-PP (dento-alveolar height in the U1 region) | The perpendicular distance between U1 and the PP. |
| U5-PP (dento-alveolar height in the U5 region) | The perpendicular distance between left and right U5 and the PP. |
| U7-PP (dento-alveolar height in the U7 region) | The perpendicular distance between left and right U7 and the PP. |
| MdL (mandibular body length) | The distance between left and right Go and Me along the MSRP. |
| Cd-Pog | The distance between left and right Cd and Pog along the MSRP. |
| CdR-VRP, CdL-VRP | The perpendicular distance between Cd and the VRP along the MSRP. |
| CdR-MSRP, CdL-MSRP | The perpendicular distance between left and right Cd and the MSRP. |
| CdR-HRP, CdL-HRP | The perpendicular distance between left and right Cd and the HRP. |
| CdR-GoR, CdL-GoL (ramus height) | The distance between left and right Cd and Go. |
| Cd-Length (Condyle length) | The distance between left and right CdLP and CdMP. |
| Cd-Width (Condyle width) | The distance between left and right CdAP and CdPP. |
| CCoR-CCoL (intercondylar distance) | Distance between the right and the left CCo along the transverse axis. |
| CCo-L1 | The distance between left and right CCo and L1 along the anteroposterior-axis. |

**Table 4.** Assess the intra-observer reproducibility.

| *Variable* | *Dalhberg* | *Houston* | *P* |
|---|---|---|---|
| MdL Shifted side | 0,33 | 0,84 | 0,1 |
| MdL Contralateral side | 0,43 | 0,84 | 0,39 |
| AOP Shifted side | 0,88 | 0,85 | 0,45 |
| AOP Contralateral side | 0,95 | 0,83 | 0,96 |
| POP Shifted side | 0,32 | 0,99 | 0,74 |
| POP Contralateral side | 0,39 | 0,86 | 0,17 |
| CCo-L1 Shifted side | 0,13 | 0,89 | 0,28 |
| CCo-L1 Contralateral side | 0,42 | 0,88 | 0,63 |
| CdAxis-VRP Shifted side | 0,82 | 0,88 | 0,67 |
| CdAxis-VRP Contralateral side | 0,69 | 0,9 | 0,63 |
| Cd-Length Shifted side | 0,25 | 0,9 | 0,85 |
| Cd-Length Contralateral side | 0,65 | 0,83 | 0,61 |
| Cd-Width Shifted side | 0,14 | 0,87 | 0,55 |
| Cd-Width Contralateral side | 0,06 | 0,85 | 0,64 |
| Cd-Pog Shifted side | 0,15 | 0,96 | 0,24 |
| Cd-Pog Contralateral side | 0,99 | 0,83 | 0,77 |
| Cd-VRP Shifted side | 0,3 | 0,9 | 0,2 |
| Cd-VRP Contralateral side | 0,98 | 0,89 | 0,89 |
| Cd-MSRP Shifted side | 0,46 | 0,87 | 0,26 |
| Cd-MSRP Contralateral side | 0,99 | 0,9 | 0,89 |
| Cd-HRP Shifted side | 0,9 | 0,83 | 0,93 |
| Cd-HRP Contralateral side | 0,39 | 0,86 | 0,27 |
| U5-PP Shifted side | 0,38 | 0,87 | 0,17 |
| U5-PP Contralateral side | 0,4 | 0,9 | 0,21 |
| U7-PP Shifted side | 0,69 | 0,88 | 0,1 |
| U7-PP Contralateral side | 0,31 | 0,87 | 0,54 |
| Po-TP-VRP Shifted side | 0,85 | 0,89 | 0,71 |
| Po-TP-VRP Contralateral side | 0,93 | 0,86 | 0,1 |
| ST-MSRP Shifted side | 0,25 | 0,84 | 0,9 |
| ST-MSRP Contralateral side | 0,64 | 0,89 | 0,77 |
| TP-MSRP Shifted side | 0,69 | 0,85 | 0,31 |
| TP-MSRP Contralateral side | 0,1 | 0,87 | 0,21 |
| TP-ST-MSRP Shifted side | 0,61 | 0,84 | 0,51 |
| TP-ST-MSRP Contralateral side | 0,99 | 0,84 | 0,26 |
| RamHt Shifted side | 0,47 | 0,99 | 0,63 |
| RamHt Contralateral side | 0,45 | 0,99 | 0,65 |
| Go-Cant | 0,34 | 0,94 | 0,63 |
| POP-Cant | 0,46 | 0,94 | 0,87 |
| AOP-Cant | 0,43 | 0,84 | 0,62 |
| Ma-Cant | 0,52 | 0,84 | 0,84 |

| | | | |
|---|---|---|---|
| MLD | 0,41 | 0,98 | 0,61 |

**Table 5.**

| Occlusal Plane and Dental Height Average Measurements | *MLD* | | | |
|---|---|---|---|---|
| | *Shifted side* | *Contralateral side* | *Difference* | *P* |
| AOP | 6.95±4.42 | 5.17±4.15 | *1.78±4.8 | 0,024 |
| POP | 15.36±4.96 | 10.59±5.17 | **4.76±3.54 | 0,000 |
| U5-PP | 24.45±3.31 | 25.61±3.01 | **-1.16±2.65 | 0,009 |
| U7-PP | 19.36±4.13 | 22.41±3.27 | **-3.1±2.33 | 0,000 |
| **Mandibular Posture Average Measurements** | *MLD* | | | |
| | *Shifted side* | *Contralateral side* | *Difference* | *P* |
| MdL | 76.1±6.87 | 73.29±6.57 | **2.81±5.2 | 0,001 |
| Cd-Pog | 121.38±9.29 | 126.73±7.28 | **-5.34±6.08 | 0,000 |
| RamHt | 56.14±7.21 | 60.01±6.59 | **-3.87±5.11 | 0,000 |
| Cd-VRP | 10.03±2.83 | 9.31±2.24 | 0.72±2.7 | 0,099 |
| Cd-MSRP | 47.38±2.68 | 50.4±3.14 | **-3.02±2.17 | 0,000 |
| Cd-HRP | 16.24±3.14 | 15.34±3.43 | 0.91±3.69 | 0,129 |
| **Condyle Average Measurements** | *MLD* | | | |
| | *Shifted side* | *Contralateral side* | *Difference* | *P* |
| CCo-L1 | 92.79±6.14 | 92.59±5.39 | 0.2±3.37 | 0,716 |
| CdAxis-VRP | 21.53±11.12 | 22.32±9.53 | -1.33±13.9 | 0,548 |
| Cd-Length | 16.81±2.86 | 18.47±2.73 | **-1.66±2.35 | 0,000 |
| Cd-Width | 6.87±1.46 | 8.44±1.59 | **-1.57±1.93 | 0,000 |
| CCo-CCo Distance | 96.32±5.53 | | | |
| **Temporal Bone Posture Average Measurements** | *MLD* | | | |
| | *Shifted side* | *Contralateral side* | *Difference* | *P* |
| TP-ST-MSRP | 29.86±11.76 | 29.25±10.3 | 0.61±6.57 | 0,561 |
| TP-MSRP | 62.43±4.5 | 60.5±4.11 | **1.93±4.28 | 0,007 |
| ST-MSRP | 47.96±5.15 | 46.08±4.07 | **1.87±4.1 | 0,006 |
| Po-TP-VRP | 26,69±6,39 | 29,98±6,16 | **-3.29±7 | 0,005 |

*Significantly different from Contralateral Side at P<0.05 level

**Significantly different from Contralateral Side at P<0.01 level

**Table 6.** Associations tested

| *Association* | *Correlation coefficient ( r )* | *P-value* |
|---|---|---|
| AOP-Cant and MLD | 0.514* | 0,001 |
| POP-Cant and MLD | 0.822* | 0,000 |
| Go-Cant and MLD | 0.833* | 0,000 |
| POP-Cant and Go-Cant | 0.835* | 0,000 |
| Ma-cant and MLD | -0.787* | 0,000 |
| POP-Cant and Ma-cant | -0.613** | 0,000 |

*P<0.01 (Spearman's coefficient (test)).
**P< 0.01 (Pearson product-moment correlation coefficient).

**Table 7.** Angle Classsification on the Shifted side and on the Contralateral side

| *Shifted side* | *n* | *Angle Classification* | *n* |
|---|---|---|---|
| Left | 21 | R-III | 7 |
| | | B-III,R>L | 7 |
| | | L-II | 5 |
| | | I | 2 |
| Right | 19 | L-III | 9 |
| | | B-III,L>R | 2 |
| | | R-II | 7 |
| | | I | 1 |

I, II, III represents Class I, Class II, Class III, respectively

R, L and B represents right, left and bilateral, respectively

**Figure legends:**

**Fig 1.** Graphic representation of the 3D planes. Reference planes are 1, 2, 3 and 4, and constructed 3D planes are 5, 6 and 7. 1, Mid-saggital reference plane (MSRP); 2, Frontal reference plane (FRP); 3, Horizontal reference plane (HRP); 4, Vertical reference plane (VRP); 5, Frankfort horizontal plane (FH); 6, Anterior occlusal plane (AOP); 7, Posterior occlusal plane (POP).

**Fig 2.** Measurement from the 3D frontal view in MLD subjects: AOP-cant, POP-cant, anterior occlusal plane cant and posterior occlusal plane cant; Go-cant, gonial cant; Ma-cant, mastoid cant.

**Fig 3.** View of the coronal CT slice of the tomographic volume at the same level as the vertical reference plane (VRP) representing the 3D measurement of frontal temporal bone inclination and temporal bone points distance. MSRP, mid-saggital reference plane; TPr and TPl, right and left tempo-parietal points; STr and STl, right and left spheno-temporal points; a and b, right and left temporal bone frontal (medial／lateral) inclination angles (TP-ST-MSRP); c-f, temporal bone point distance (TPr-MSRP, TPl-MSRP, STr-MSRP, STl-MSRP , respectively).

**Fig 4.** Definition of temporal bone sagittal inclination. VRP, vertical reference plane; TPr, right temporal point; Por, right porion; 1, temporal anterior／posterior inclination angle (Po-TP-VRP).

**Fig 5.** Lateral view with the presence of the median sagittal tomographic volume slice. ANS, anterior nasal spine; PNS, posterior nasal spine; a, 21; b, 15／25; c, 17／27; FH, Frankfort horizontal plane; PP, palatal plane; AOP, anterior occlusal plane (between landmarks 21 and 15／25; inclination of this line was calculated relative to FH plane); POP, posterior occlusal plane (between landmarks 15／25 and 17／27; inclination of this line was calculated relative to FH plane); d–f, maxillary dento-alveolar height (17／27-PP, 15／25-PP and 21-PP, respectively).

**Fig 6.** Landmarks for measuring three-dimensional structure of the condyle. **A**, Most central point from a lateral view of the condyle. **B**, Frontal view of the mid-point between most lateral (L) and most medial convex point (M). **C**, Superior view of the mid-point between lateral, medial, anterior (A) and posterior (P) convex point; 1, condyle length (from M point to L point); 2, condyle width (from A point to P point). Arrows indicate landmark.

**Fig 7.** Measurement angle formed by the Bonwill triangle, which consisted of both right and left central condyle point (CCo) and lower incisal points (L1).

**Fig 8.** Measurements of the condyle posture. MSRP, mid-saggital reference plane; VRP, vertical reference plane; HRP, horizontal reference plane. Cdr and Cdl, right and left condylion point; condylion point distance (Cd_r-MSRP, Cd_r-VRP, Cd_r-HRP, Cd_l-MSRP, Cd_l-VRP, Cd_l-HRP respectively).

**Fig 9.** Lateral view of mandibular measurement. a, Cd; b, Go; c, Pog; 1, (Cd-Go); 2, (Go-Pog); 3, (Cd-Pog).

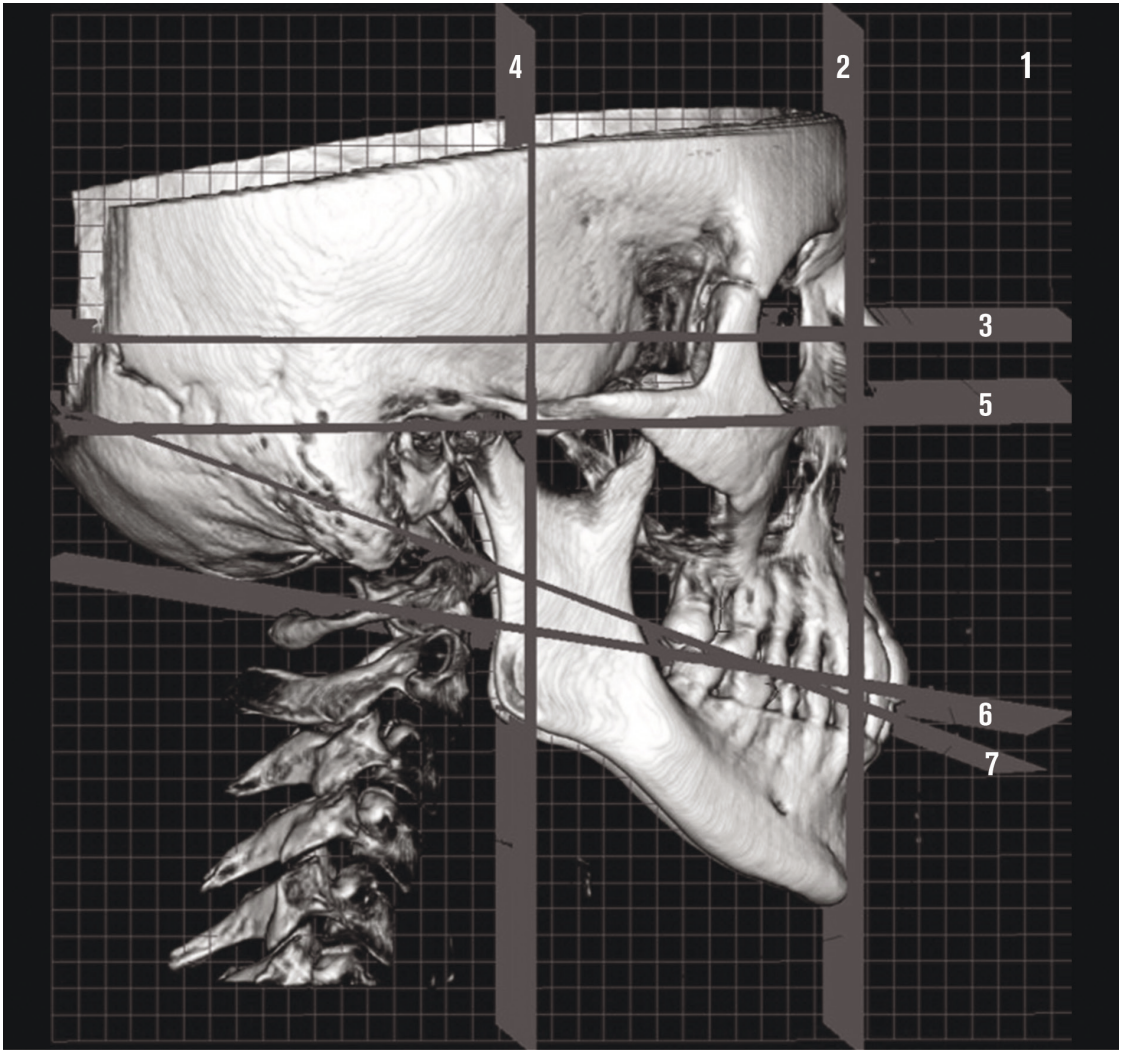
4
2
1
3
5
6
7

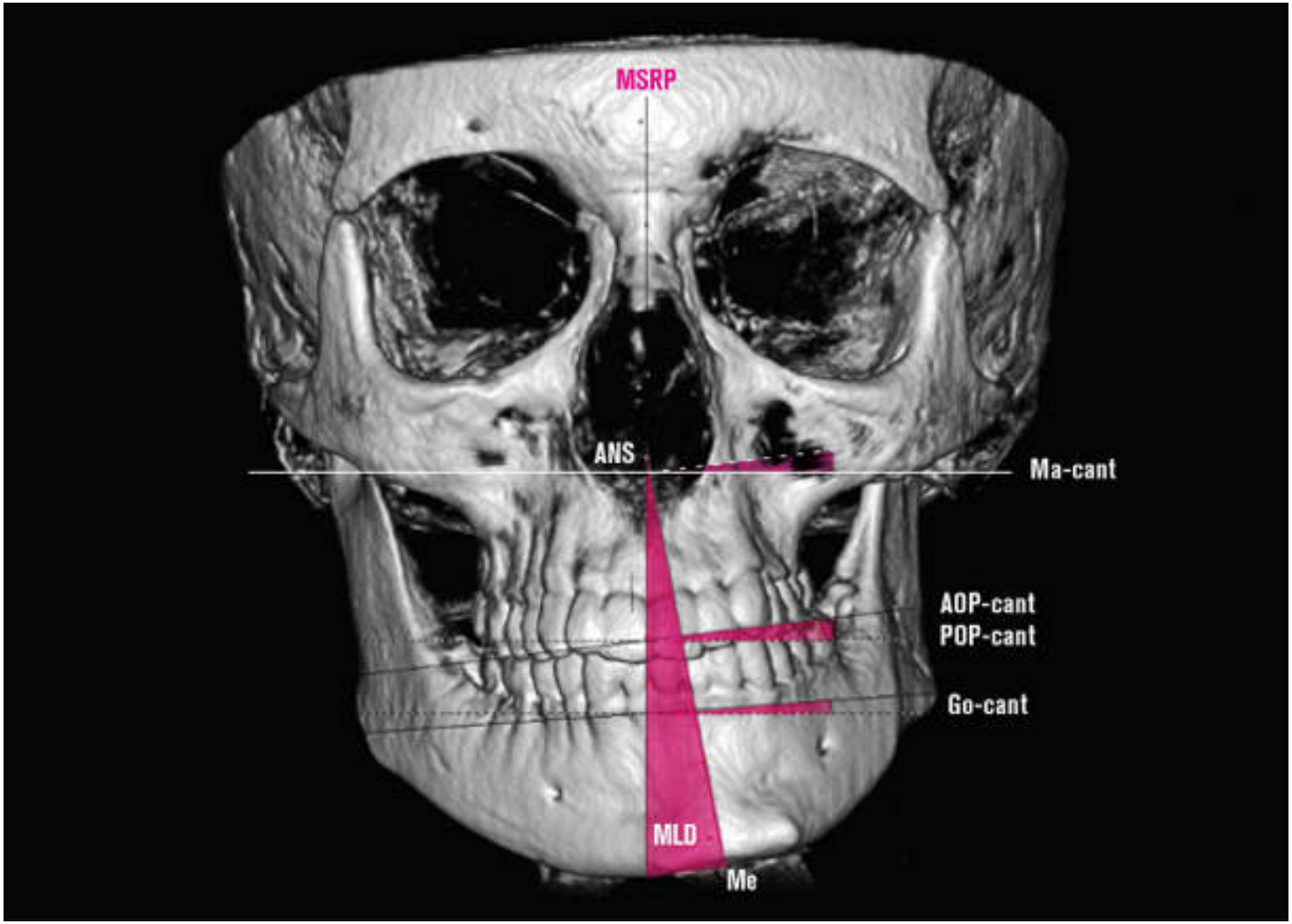
MSRP
ANS
Ma-cant
AOP-cant
POP-cant
Go-cant
MLD
Me

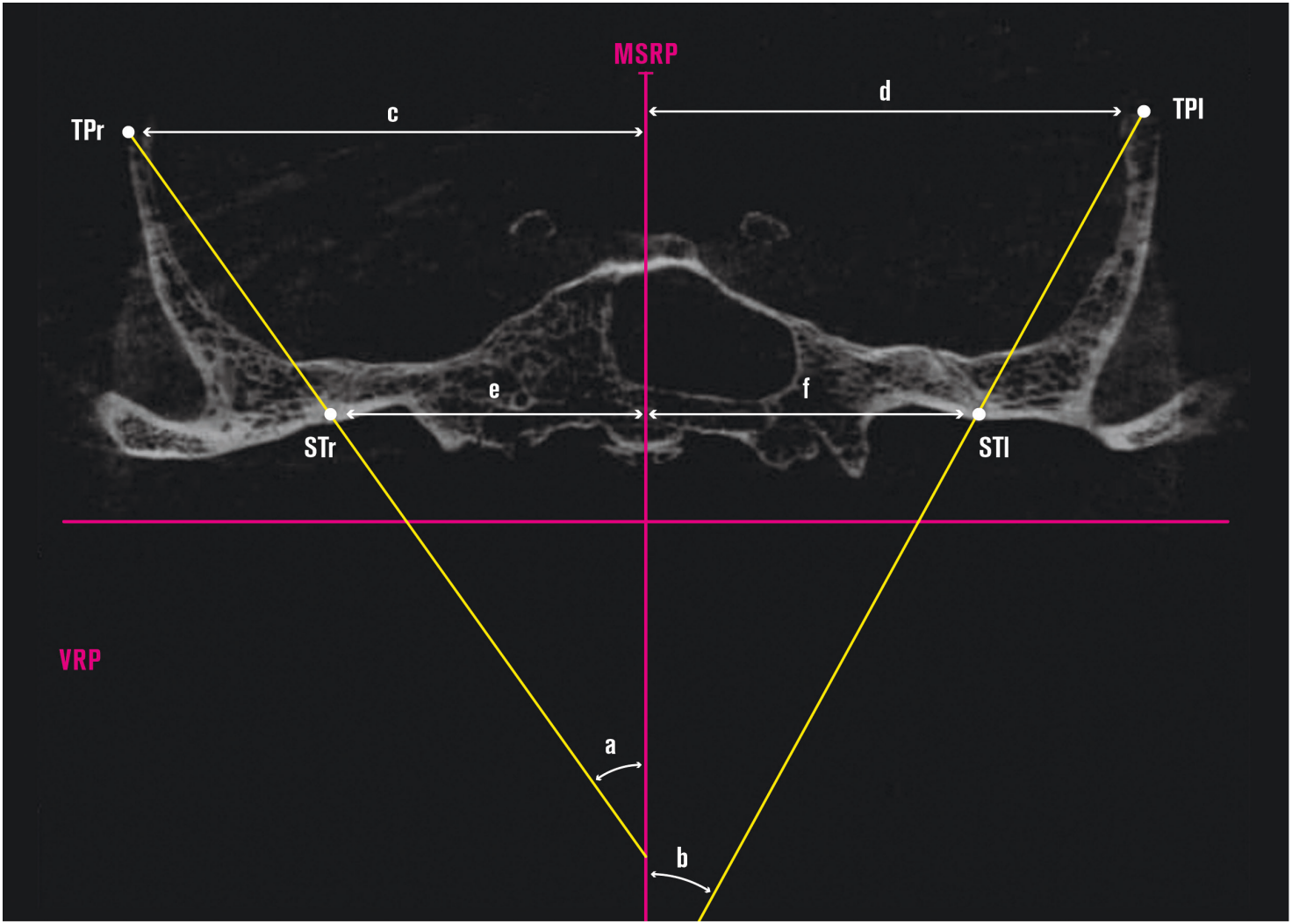
MSRP
TPr
c
d
TPl
e
f
STr
STl
VRP
a
b

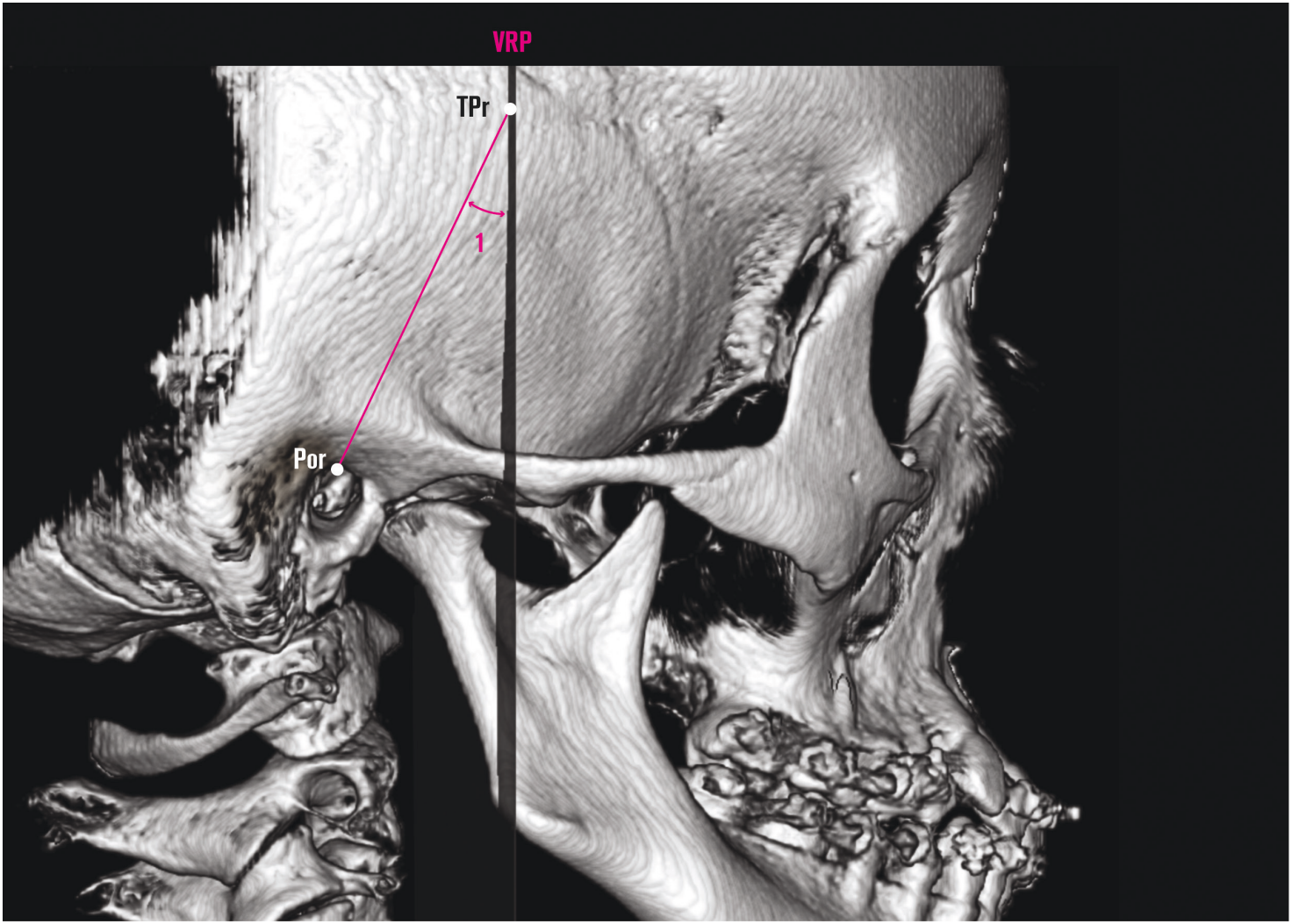
VRP
TPr
1
Por

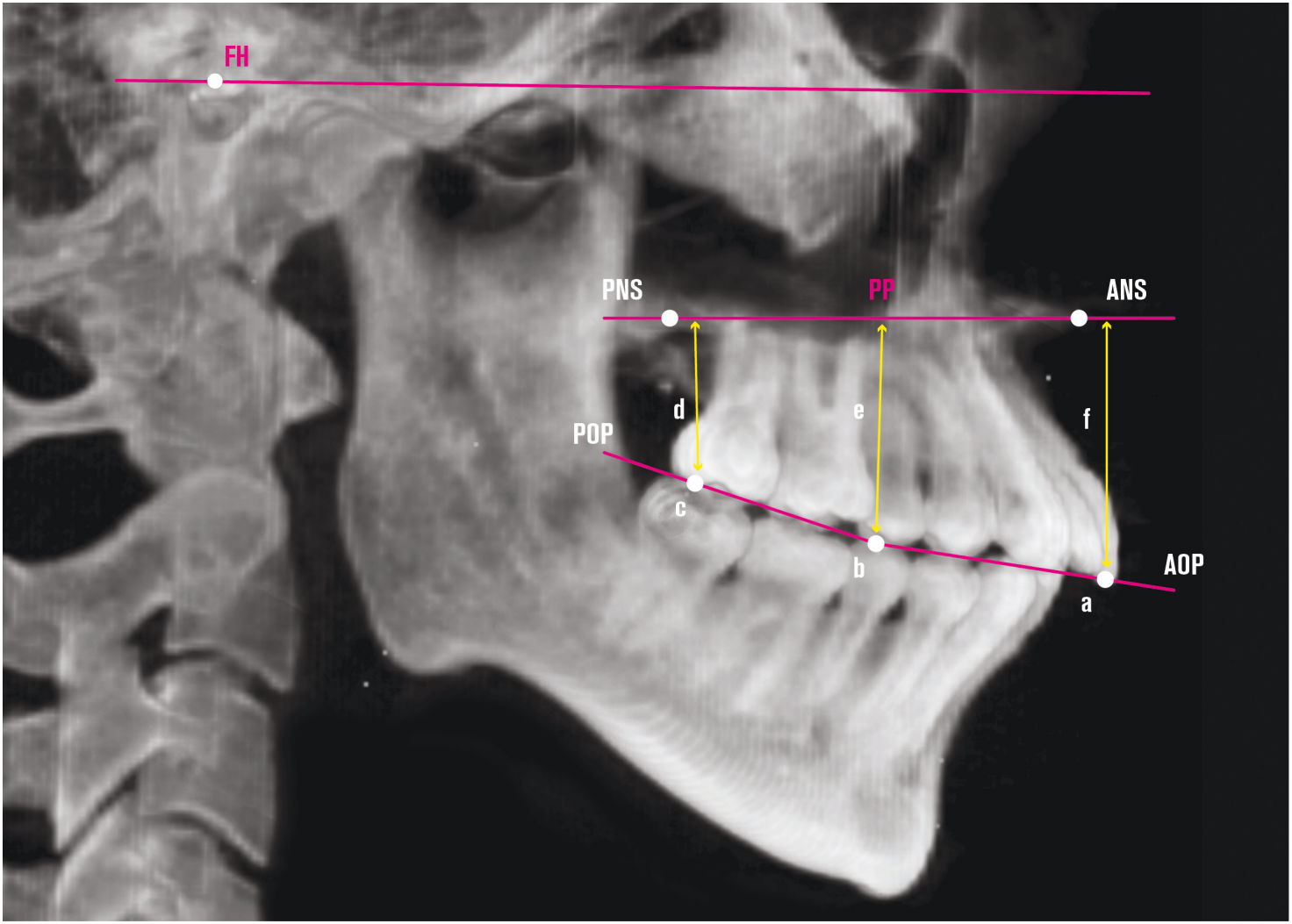
FH
PNS
PP
ANS
d
e
f
POP
c
b
AOP
a

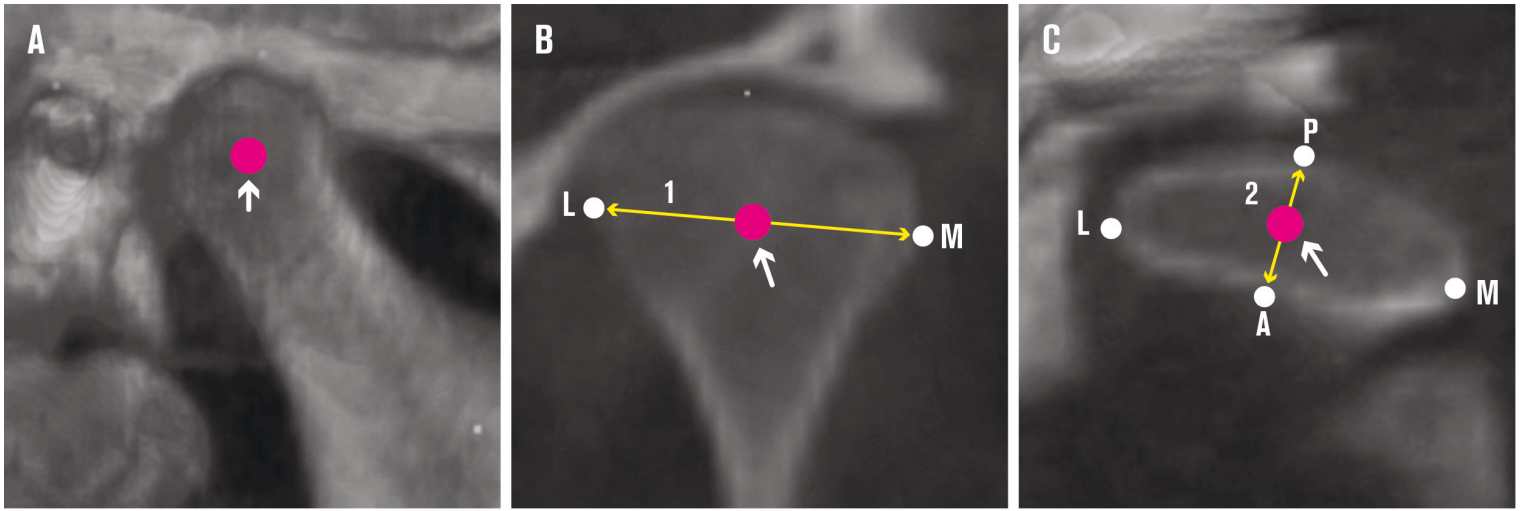
A
B
L
1
M
C
P
2
L
A
M

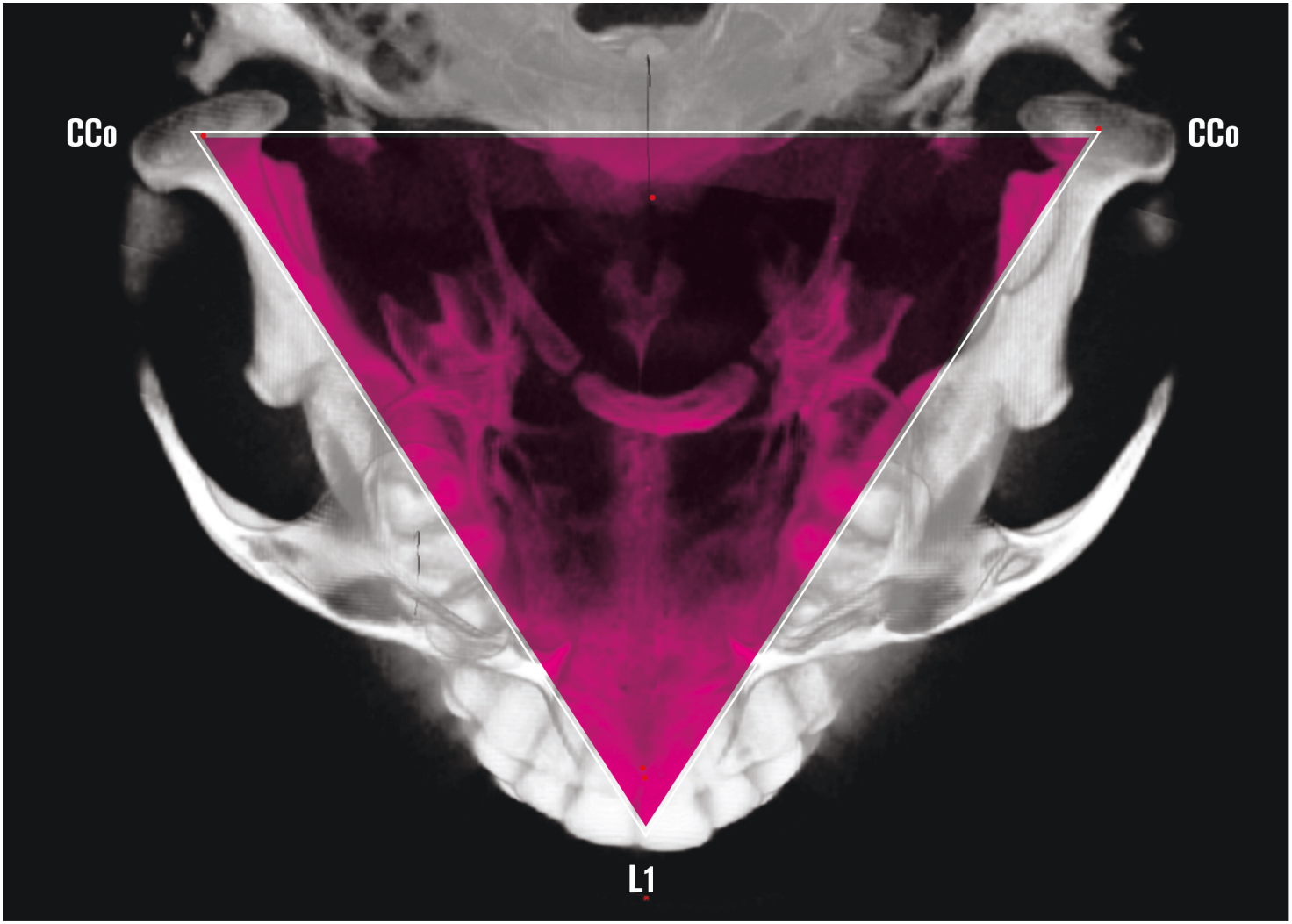
CCo
CCo
L1

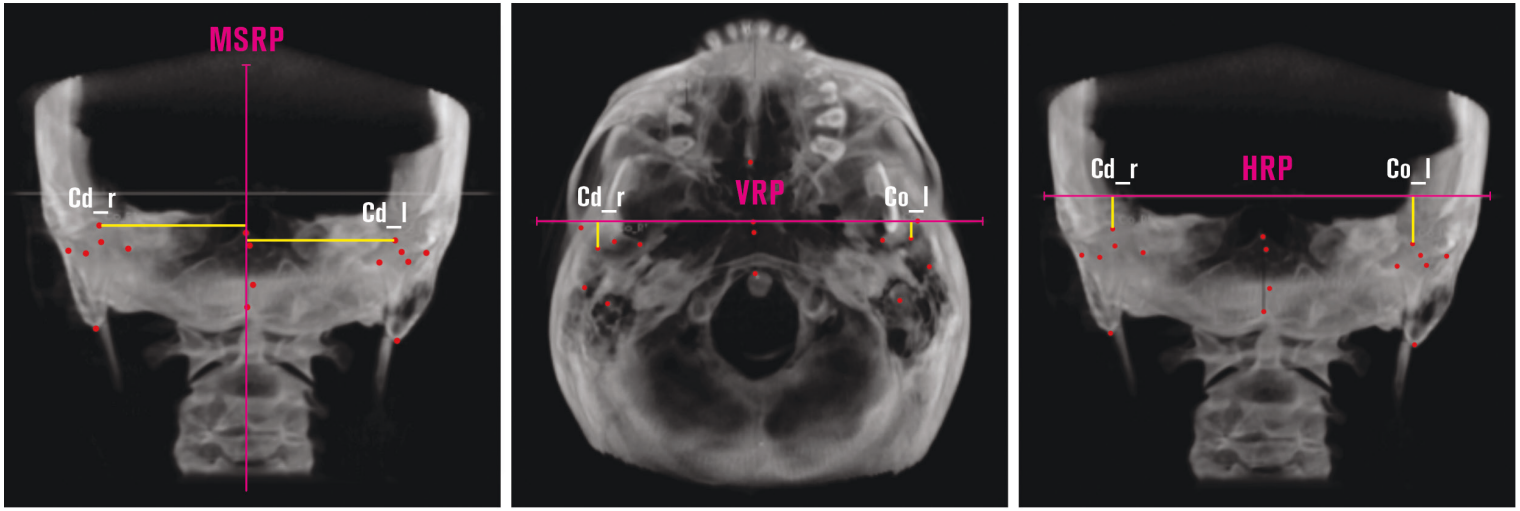
MSRP
Cd_r
Cd_l
Cd_r
VRP
Co_l
Cd_r
HRP
Co_l

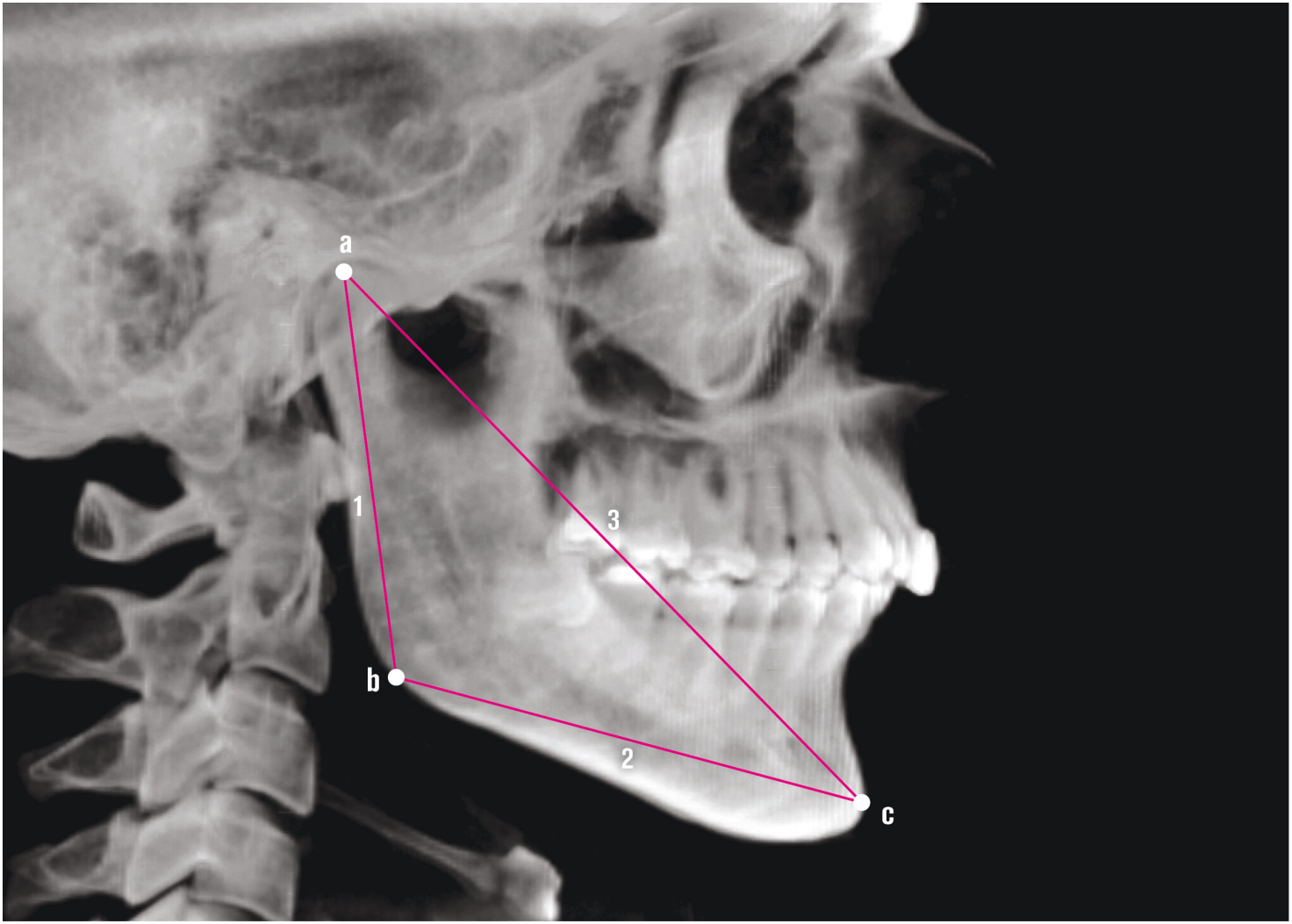
a
1
3
b
2
c

**Table 1.** Description of the 3D cephalometric landmarks used in this study.

| *Landmark* | *Definition* |
|---|---|
| S (Sella) | The midpoint of the pituitary fossa in the midsagittal plane. |
| N (Nasion) | The middle point of the frontonasal suture in the frontal plane. |
| Ba (Basion) | Anterior-inferior margin of the foramen magnum. |
| PoR-PoL (Porion) | Most superior point of the right (PoR) and left (PoL) outer acoustic |
| OrR-OrL (Orbital) | The most inferior point on the infraorbital rim of the maxilla. |
| STR, STL (Sphenotemporal point) | The most anterior point on the external surface of the right (STR) and left (STL) sphenotemporal suture. |
| TPR, TPL (Temporoparietal point) | The most superior point on the external surface of the right (TPR) and left (TPL) temporoparietal suture. |
| MaR-MaL (Mastoid) | The lowest point of the mastoid process of the temporal bone. |
| ANS (Anterior nasal spine) | The most anterior point of the premaxillary bone in the sagittal plane. |
| PNS (Posterior nasal spine) | The most posterior point of the palatine bone in the midsagittal plane. |
| A (A point) | The deepest point in the anterior outline of the maxilla between supradentale and ANS in the midsagittal plane. |
| U1 (Upper interincisor point) | The most incisal point between the two upper central incisors. |
| U5R, U5L (2nd premolar) | Tip of the buccal cusp of the second upper right (U5R) and left (U5L) |
| Premed (Mean 2nd premolar) | Calculated 3D medial (mean) point between U5R and U5L. |
| U7R, U7L (2nd molar) | Tip of the distobuccal cusp of the upper right (U7R) and left (U7L) second molar. |
| B (B point) | The deepest point in the anterior outline of the mandible between infradentale and pogonion in the sagittal plane. |
| Pg (Pogonion) | The most anterior point in the mandibular chin area in the sagittal |
| Me (Menton) | The most inferior point in the mandibular chin area in the sagittal plan. |
| GoR and GoL (Gonion) | The midpoint of the right (GoR) and left (GoL) angles of the mandible, formed by the inferior border of the corpus and posterior ramus border. |
| CdR-CdL (Condylion) | Most posterosuperior point of the right (CdR) and left (CdL) mandibular condyle. |
| CdLR-CdLL (Condylion lateral pole) | The most lateral point of the right (CdLR) and left (CdLL) condylar |
| CdMR-CdML (Condylion medial pole) | The most medial point of the right (CdLR) and left (CdLL) condylar |
| CdAR-CdAL (Condylion anterior pole) | The most anterior point of the right (CdLR) and left (CdLL) condylar |
| CdPR-CdPL (Condylion posterior pole) | The most posterior point of the right (CdLR) and left (CdLL) condylar |
| CCoR-CCoL (Center of condyle) | The 3D central point of the right (CCoR) and left (CCoL) mandibular condyle |
| L1 (lower interincisor point) | The most incisal point between the two lower central incisors. |

**Table 2.** Definition of 3D planes used in the analysis

| *Plane* | *Definition* |
|---|---|
| MSRP (Midsagittal reference plane) | Plane through Basion, Nasion, and ANS. |
| AH (Anatomical Horizontal) | Plane that contains posterior – anterior vector (PoR to OrR) that is perpendicular to the midsagittal reference plane (MSRP) |
| FRP (Frontal reference plane) | Plane through Nasion and perpendicular to the midsagittal reference plane (MSRP) and anatomical |
| HRP (Horizontal reference plane) | Plane through Sella and perpendicular to the midsagittal reference plane (MSRP) and frontal reference |
| VRP (Vertical reference plane) | Plane through Sella and perpendicular to the midsagittal reference plane (MSRP) and anatomical |
| AOP (Anterior occlusal plane) | premolar. |
| POP (Posterior occlusal plane) | molar. |

**Table 3.** Definition of the Cephalometric angular and linear measurements used in this study.

| *Measurement* | *Definition* |
|---|---|
| Angular measurements: | |
| STTP-MSRP (temporal frontal inclination) | Mean angle between left and right ST-TP lines and the midsagittal reference plane (MSRP). |
| PoTP-VRP (temporal sagittal inclination) | Mean angle between left and right Po-TP lines and the vertical reference plane (VRP). |
| AOPL-FH | 3D angle between AOPL and FH reference plane. |
| AOPR-FH | 3D angle between AOPR and FH reference plane. |
| POPL-FH | 3D angle between POPL and FH reference plane. |
| POPR-FH | 3D angle between POPR and FH reference plane. |
| CdAxis-VRP | Mean angle between left (CdLL-CdML) and right (CdLR-CdMR) |
| MLD (mandibular lateral displacement) | ANS-Men line and MSRP (Ba-Na-ANS) |
| Go-cant (gonial cant) | 3D angle between GoR-GoL line and FH reference plane |
| Ma-cant (mastoid cant) | 3D angle between MaR-MaL line and FH reference plane |
| Linear measurements: | |
| ST-MSRP | The perpendicular distance between left and right ST and the MSRP. |
| TP-MSRP | The perpendicular distance between left and right TP and the MSRP. |
| U1-PP (dento-alveolar height in the U1 region) | The perpendicular distance between U1 and the PP. |
| U5-PP (dento-alveolar height in the U5 region) | The perpendicular distance between left and right U5 and the PP. |
| U7-PP (dento-alveolar height in the U7 region) | The perpendicular distance between left and right U7 and the PP. |
| MdL (mandibular body length) | The distance between left and right Go and Me along the MSRP. |
| Cd-Pog | The distance between left and right Cd and Pog along the MSRP. |
| CdR-VRP, CdL-VRP | The perpendicular distance between Cd and the VRP along the MSRP. |
| CdR-MSRP, CdL-MSRP | The perpendicular distance between left and right Cd and the MSRP. |
| CdR-HRP, CdL-HRP | The perpendicular distance between left and right Cd and the HRP. |
| CdR-GoR, CdL-GoL (ramus height) | The distance between left and right Cd and Go. |
| Cd-Length (Condyle length) | The distance between left and right CdLP and CdMP. |
| Cd-Width (Condyle width) | The distance between left and right CdAP and CdPP. |
| CCoR-CCoL (intercondylar distance) | Distance between the right and the left CCo along the transverse axis. |
| CCo-L1 | The distance between left and right CCo and L1 along the anteroposterior-axis. |

**Table 4.** Assess the intra-observer reproducibility.

| *Variable* | *Dalhberg* | *Houston* | *P* |
|---|---|---|---|
| MdL Ipsilateral side | 0.33 | 0.84 | 0.1 |
| MdL Contralateral side | 0.43 | 0.84 | 0.39 |
| AOP Ipsilateral side | 0.88 | 0.85 | 0.45 |
| AOP Contralateral side | 0.95 | 0.83 | 0.96 |
| POP Ipsilateral side | 0.32 | 0.99 | 0.74 |
| POP Contralateral side | 0.39 | 0.86 | 0.17 |
| CCo-L1 Ipsilateral side | 0.13 | 0.89 | 0.28 |
| CCo-L1 Contralateral side | 0.42 | 0.88 | 0.63 |
| CdAxis-VRP Ipsilateral side | 0.82 | 0.88 | 0.67 |
| CdAxis-VRP Contralateral side | 0.69 | 0.9 | 0.63 |
| Cd-Length Ipsilateral side | 0.25 | 0.9 | 0.85 |
| Cd-Length Contralateral side | 0.65 | 0.83 | 0.61 |
| Cd-Width Ipsilateral side | 0.14 | 0.87 | 0.55 |
| Cd-Width Contralateral side | 0.06 | 0.85 | 0.64 |
| Cd-Pog Ipsilateral side | 0.15 | 0.96 | 0.24 |
| Cd-Pog Contralateral side | 0.99 | 0.83 | 0.77 |
| Cd-VRP Ipsilateral side | 0.3 | 0.9 | 0.2 |
| Cd-VRP Contralateral side | 0.98 | 0.89 | 0.89 |
| Cd-MSRP Ipsilateral side | 0.46 | 0.87 | 0.26 |
| Cd-MSRP Contralateral side | 0.99 | 0.9 | 0.89 |
| Cd-HRP Ipsilateral side | 0.9 | 0.83 | 0.93 |
| Cd-HRP Contralateral side | 0.39 | 0.86 | 0.27 |
| U5-PP Ipsilateral side | 0.38 | 0.87 | 0.17 |
| U5-PP Contralateral side | 0.4 | 0.9 | 0.21 |
| U7-PP Ipsilateral side | 0.69 | 0.88 | 0.1 |
| U7-PP Contralateral side | 0.31 | 0.87 | 0.54 |
| Po-TP-VRP Ipsilateral side | 0.85 | 0.89 | 0.71 |
| Po-TP-VRP Contralateral side | 0.93 | 0.86 | 0.1 |
| ST-MSRP Ipsilateral side | 0.25 | 0.84 | 0.9 |
| ST-MSRP Contralateral side | 0.64 | 0.89 | 0.77 |
| TP-MSRP Ipsilateral side | 0.69 | 0.85 | 0.31 |
| TP-MSRP Contralateral side | 0.1 | 0.87 | 0.21 |
| TP-ST-MSRP Ipsilateral side | 0.61 | 0.84 | 0.51 |
| TP-ST-MSRP Contralateral side | 0.99 | 0.84 | 0.26 |
| RamHt Ipsilateral side | 0.47 | 0.99 | 0.63 |
| RamHt Contralateral side | 0.45 | 0.99 | 0.65 |

| | | | |
|---|---|---|---|
| Go-Cant | 0.34 | 0.94 | 0.63 |
| POP-Cant | 0.46 | 0.94 | 0.87 |
| AOP-Cant | 0.43 | 0.84 | 0.62 |
| Ma-Cant | 0.52 | 0.84 | 0.84 |
| MLD | 0.41 | 0.98 | 0.61 |

**Table 5.**

| Occlusal Plane and Dental Height Average Measurements | *MLD* | | | |
|---|---|---|---|---|
| | *Shifted side* | *Contralateral side* | *Difference* | *P* |
| AOP | 6.95±4.42 | 5.17±4.15 | *1.78±4.8 | 0.024 |
| POP | 15.36±4.96 | 10.59±5.17 | **4.76±3.54 | 0.000 |
| U5-PP | 24.45±3.31 | 25.61±3.01 | **-1.16±2.65 | 0.009 |
| U7-PP | 19.36±4.13 | 22.41±3.27 | **-3.1±2.33 | 0.000 |
| **Mandibular Posture Average Measurements** | *MLD* | | | |
| | *Shifted side* | *Contralateral side* | *Difference* | *P* |
| MdL | 76.1±6.87 | 73.29±6.57 | **2.81±5.2 | 0.001 |
| Cd-Pog | 121.38±9.29 | 126.73±7.28 | **-5.34±6.08 | 0.000 |
| RamHt | 56.14±7.21 | 60.01±6.59 | **-3.87±5.11 | 0.000 |
| Cd-VRP | 10.03±2.83 | 9.31±2.24 | 0.72±2.7 | 0.099 |
| Cd-MSRP | 47.38±2.68 | 50.4±3.14 | **-3.02±2.17 | 0.000 |
| Cd-HRP | 16.24±3.14 | 15.34±3.43 | 0.91±3.69 | 0.129 |
| **Condyle Average Measurements** | *MLD* | | | |
| | *Shifted side* | *Contralateral side* | *Difference* | *P* |
| CCo-L1 | 92.79±6.14 | 92.59±5.39 | 0.2±3.37 | 0.716 |
| CdAxis-VRP | 21.53±11.12 | 22.32±9.53 | -1.33±13.9 | 0.548 |
| Cd-Length | 16.81±2.86 | 18.47±2.73 | **-1.66±2.35 | 0.000 |
| Cd-Width | 6.87±1.46 | 8.44±1.59 | **-1.57±1.93 | 0.000 |
| CCo-CCo Distance | 96.32±5.53 | | | |
| **Temporal Bone Posture** | *MLD* | | | |

| Average Measurements | *Shifted side* | *Contralateral side* | *Difference* | *P* |
|---|---|---|---|---|
| TP-ST-MSRP | 29.86±11.76 | 29.25±10.3 | 0.61±6.57 | 0.561 |
| TP-MSRP | 62.43±4.5 | 60.5±4.11 | **1.93±4.28 | 0.007 |
| ST-MSRP | 47.96±5.15 | 46.08±4.07 | **1.87±4.1 | 0.006 |
| Po-TP-VRP | 26,69±6,39 | 29,98±6,16 | **-3.29±7 | 0.005 |

*Significantly different from Contralateral Side at P<0.05 level

**Significantly different from Contralateral Side at P<0.01 level

**Table 6. Associations tested**

| *Association* | *Correlation coefficient ( r )* | *P-value* |
|---|---|---|
| AOP-Cant and MLD | 0.514* | 0.001 |
| POP-Cant and MLD | 0.822* | 0.000 |
| Go-Cant and MLD | 0.833* | 0.000 |
| POP-Cant and Go-Cant | 0.835* | 0.000 |
| Ma-cant and MLD | -0.787* | 0.000 |
| POP-Cant and Ma-cant | -0.613** | 0.000 |

*P<0.01 (Spearman's coefficient (test)).

**P< 0.01 (Pearson product-moment correlation coefficient).

**Table 7.** Angle Classsification on the Shifted side and on the Contralateral side

| *Shifted side* | *n* | *Angle Classification* | *n* |
|---|---|---|---|
| Left | 21 | R-III | 7 |
| | | B-III,R>L | 7 |
| | | L-II | 5 |
| | | I | 2 |
| Right | 19 | L-III | 9 |
| | | B-III,L>R | 2 |
| | | R-II | 7 |
| | | I | 1 |

I, II, III represents Class I, Class II, Class III, respectively

R, L and B represents right, left and bilateral, respectively